Volume 30 | Number 12 | December 2015 | Pages 2361–2556

JAAS

Journal of Analytical Atomic Spectrometry

www.rsc.org/jaas

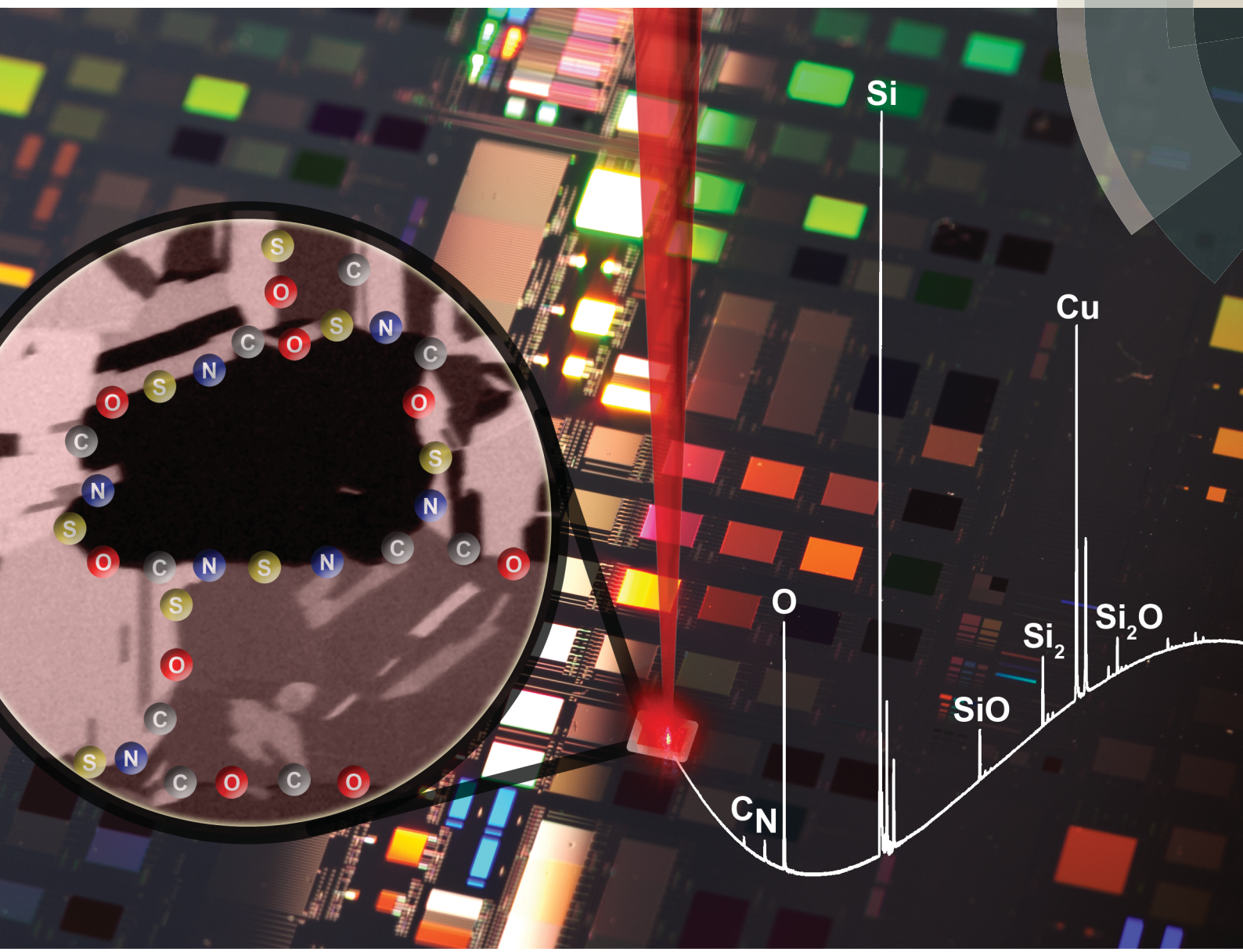

ISSN 0267-9477

ROYAL SOCIETY OF CHEMISTRY

COMMUNICATION

A. Riedo *et al.*

High depth-resolution laser ablation chemical analysis of additive-assisted Cu electroplating for microchip architectures

JAAS

COMMUNICATION

View Article Online
View Journal | View Issue

Cite this: J. Anal. At. Spectrom., 2015, 30, 2371

Received 21st July 2015
Accepted 14th October 2015

DOI: 10.1039/c5ja00295h

www.rsc.org/jaas

High depth-resolution laser ablation chemical analysis of additive-assisted Cu electroplating for microchip architectures

A. Riedo,*[a] V. Grimaudo,[b] P. Moreno-García,[b] M. B. Neuland,[a] M. Tulej,[a] P. Wurz[a] and P. Broekmann[b]

Laser ablation/ionisation mass spectrometry with a vertical resolution at a nanometre scale was applied for the quantitative characterisation of the chemical composition of additive-assisted Cu electroplated deposits used in the microchip industry. The detailed chemical analysis complements information gathered by optical techniques and allows new insights into the metal deposition process.

Copper technology is a key element for the fabrication of state-of-the-art logic and memory devices.[1] An additive-assisted copper electroplating process is typically employed to fill trenches and vias on patterned Si-wafers with copper.[2] Current challenges concern both extremely small (Damascene) features reaching the sub-10 nm regime[3,4] and extremely large, high-aspect ratio interconnects, so-called Through Silicon Vias (TSVs).[5] The latter are becoming increasingly important for the on-chip 3D integration of logic and memory devices. It is the non-uniform coverage of both inhibiting and accelerating additives on the patterned wafer surface that drives the required bottom-up fill of Damascene and TSV features with copper. Geometric shape evolution effects upon bottom-up fill[2] in conjunction with particular additive transport and adsorption kinetics[6] have been identified as physical origins of the desired bottom-up fill mechanism. An undesired side effect of the use of additives is, however, their (partial) inclusion into the interconnect material upon fill. Contaminations at the ppm level are already sufficient to decelerate the post-deposition recrystallisation of copper,[7] which is required to reach the necessary electrical conductivity of the interconnect material. Furthermore, the presence of contaminants inside the interconnect lines is a major drawback causing defects (voiding) to appear during the operation of the semiconductor device thereby lowering its overall life-time. A current challenge, not only in copper technology but in all scientific and technological fields dealing with the fabrication of ultra-clean functional materials, is the qualitative determination of embedded contaminants and their spatially resolved quantification. Challenges related to the copper technology discussed herein can be considered as a prime-example of a more general (universal) challenge in materials science, which is addressed in the following.

For direct analysis of the chemical composition of layered materials at the sub-micrometre scale, instruments with high detection sensitivity and high spatial (lateral and vertical) resolution are mandatory. To date, a variety of different instruments have been applied in this field of research, including Auger Electron Spectroscopy (AES),[8,9] X-ray Photoelectron Spectroscopy (XPS),[8,10] Secondary Ion Mass Spectrometry (SIMS),[8,11] Glow Discharge Time-of-Flight Mass Spectrometry (GD-TOF-MS),[8,12] or Laser Ablation Inductively Coupled Plasma Mass Spectrometry (LA-ICP-MS).[8,13,14] However, these experimental techniques significantly differ in their measurement capabilities and limitations, including their detection sensitivity (*e.g.* scanning *versus* non-scanning), quantitative nature of conducted measurements (*e.g.* SIMS *versus* LA-ICP-MS), lateral and vertical profiling capabilities (*e.g.* SIMS *versus* GD-TOF-MS), measurement speed, or even limitations concerning the usable sample shape.[8] Therefore, typically a combination of several analytical techniques is necessary to address this scientific question.

In this report, we present for the first time sensitive and spatially highly resolved Laser Ablation/Ionisation Mass Spectrometry (LIMS) measurements that complement the knowledge gained from Focused Ion Beam (FIB) measurements of additive-assisted electroplating processes. The unique measurement capabilities of our LIMS system (described in the following) allow the identification and quantification of grain sized chemical inhomogeneities accumulated at the grain boundaries over a range of more than 10 μm depth inside the copper deposit. The technical details and principle of operation of the LIMS instrument used in this study have already been described extensively in previous literature,[15–22] including its capability to provide sensitive and quantitative elemental

[a]Physics Institute, Space Research and Planetary Sciences, University of Bern, Sidlerstrasse 5, CH-3012 Bern, Switzerland. E-mail: andreas.riedo@space.unibe.ch
[b]Department of Chemistry and Biochemistry, Interfacial Electrochemistry Group, University of Bern, Freiestrasse 3, CH-3012 Bern, Switzerland

analysis down the 10 ppb level,[19,20] accurate isotope measurements,[18] 2D elemental imaging of heterogeneous materials,[16,17] and high resolution depth profiling at the sub-nm scale.[15] Individual analytical and technical capabilities are found also in other techniques, but are jointly available in one single measurement in our LIMS instrument. This combination of capabilities makes our instrument a highly innovative and powerful analytical technique for the chemical analyses of layered materials. The applied LIMS technique shows, *e.g.* comparable or better depth resolution capabilities compared to SIMS/GD-MS and LA-ICP-MS, as well as significant better lateral resolution than GD-MS. The LIMS measurements are conducted in a truly quantitative manner, contrary to SIMS, they outperform spectroscopic techniques in terms of detection sensitivity and dynamic range, and the clean ablation process allows depth profiling studies over tens of micrometres without the need for any preliminary sample preparation,[15] which is beyond the measurement capabilities of typical surface analytical techniques, *e.g.* AES and XPS. A brief overview of the LIMS instrument and its operation principle is given below.

A sensitive and miniature (160 mm × Ø 60 mm) reflectron-type time-of-flight mass spectrometer using laser ablation/ionisation, originally designed for *in situ* space exploration,[22] was used for chemical analysis of the sample material. The LIMS instrument uses a pulsed laser system ($\lambda = 775$ nm, $\tau \sim 190$ fs, repetition rate ≤ 1 kHz, intensity ≤ 1 mJ per pulse) for clean ablation and ionisation of the sample material. Femtosecond laser ablation allows measurements with uniform ionisation efficiencies of most elements at minimized elemental fractionation.[19,23] Laser pulses are focused by using a lens system through an ion-optical system onto the sample surface resulting in laser ablation craters of about 15 μm in diameter. The produced ions are guided through a time-of-flight analyser and recorded with a microchannel plate detector (MCP) system followed by a data acquisition system, consisting of two high-speed digitizers (8 bit, each with 2 channels, up to 4 GS s^{-1}). A full mass spectrum, ranging from hydrogen to lead, is recorded for each laser pulse. The special design of the MCP detector system with multi-anode readout capability provides a large dynamic range of more than eight orders of magnitude and allows studying simultaneously the chemical composition of major to trace elements in the target sample material.[20]

The tunable non-linear interplay of prototypical Imep (polymerizates of epichlorohydrin and imidazole) and SPS (bis-(sodium-sulfopropyl)-disulfide) additive package for Damascene applications was used to fabricate a sample bearing spatially confined layers with sequential marginal and high additive inclusion.[24,25] The physical origin of these spatially confined layers is a so-called N-shaped negative differential resistance that, within a relatively narrow current density range, is manifested by potential oscillations during galvanostatic (constant current density, J) electrodeposition.[26,27] These potential oscillations are attributed to periodic degradation and restauration of an active suppressing film at the interface between the metal and the electrolyte upon electrochemical deposition. The resulting sample structure bearing distinguishable multiple layers perpendicular to the growth direction makes it an ideal platform for chemical depth profiling studies. A total layer thickness of 15.4 μm of Cu was electrochemically deposited at $J = -6$ mA cm^{-2} on blanked Si-wafer (Hionix, BASF), composed of a Si(100)-type substrate, covered by a 500 nm thick TO_x/SiO_2 dielectric layer, a 25 nm thick Ta/TaN barrier and a terminating 100 nm thick Cu seed layer. Further details of the sample preparation procedure can be found in ref. 15.

The potential transient corresponding to the electrochemical deposition of the Cu sample is displayed by the red solid line at the rightmost side in Fig. 1. The plot shows seven regular potential oscillations, which are attributed to the sequential formation of the stable Imep–Cu(I)–MPS suppressor film and its partial dissolution (deactivation) at the interface.[24,25] The intervals at higher overpotentials comprised between sharp potential steps correspond to an active Imep–Cu(I)–MPS diffusion barrier being operative at the interface. The abrupt decrease and the following increase of the deposition overpotential are indicative of partial or complete breakdown and subsequent restoration of the suppressor ensemble. It has been qualitatively demonstrated that the suppressing ensemble incorporates into the copper matrix to a substantial extent specifically during the sharp potential transitions and that in the course of quasi-steady state deposition, it remains almost impurity free.[11] As a consequence, post-deposition recrystallisation of such samples extends over large domains and is typically confined by the localised contamination at such sharp boundaries.

The sample described was first investigated by using laser ablation/ionisation mass spectrometry where a raster of 7 × 7 different surface locations was analysed. High-resolution depth profiling measurements were performed as discussed previously.[15] For this study, a laser irradiance of about 3.3 TW cm^{-2} was applied and about 1500 single laser shots were necessary to reach the sample substrate (corresponding to a mean depth

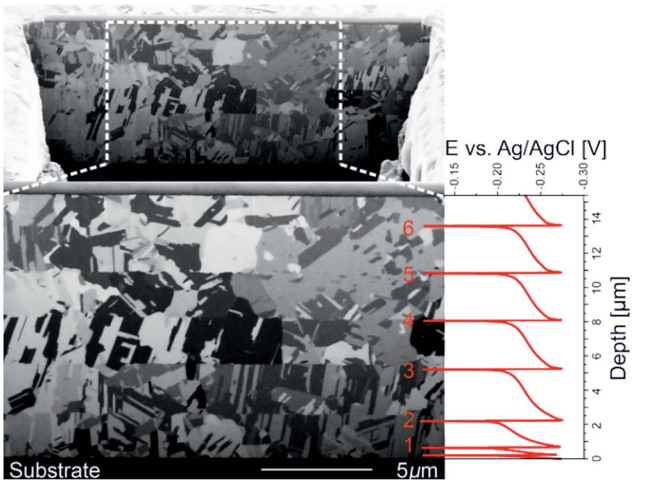

Fig. 1 FIB micrograph. The micrograph shows the cross-section of the galvanostatically electrodeposited Cu film on a Si-substrate, including the numbering of the transition layers. The right panel shows the potential *versus* depth curve from the Cu deposition (in red). The depth position of each transition layer is in good agreement with the spacing of the potential oscillations.

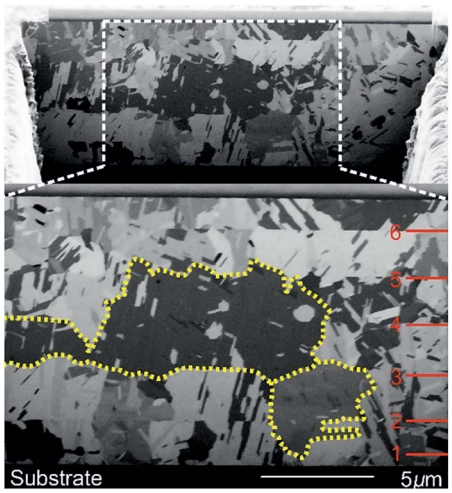

Fig. 2 FIB micrograph. The micrograph illustrates the cross-section of a second surface position on the electrodeposited Cu film. In contrast to Fig. 1, the contamination layers are less defined within this cross-section, which agrees only partially with the potential/charge oscillations in the galvanostatic measurement, marked in red.

resolution of ~10 nm per single laser shot). Subsequently, the same sample was analysed by FIB measurements conducted on two different surface locations (differing from LIMS measurement positions).

The FIB micrographs in Fig. 1 and 2 each show a cross-section of the same copper film deposited under oscillatory conditions, but measured at two different surface locations, pointing out two possible recrystallisation states within the same copper material. The first cross-section includes six transition layers (seen as sharp horizontal lines, Fig. 1) confining the recrystallisation of Cu domains, which can be assigned to the sharp increase and subsequent decrease in the overpotential *versus* the depth curve of the deposition (see red curve to the right of Fig. 1). We notice that due to the close proximity of the first two potential oscillations only six such boundaries are observed in the FIB micrograph (see Fig. 1). The agreement between the potential transient and the FIB micrograph holds only partly for the second investigated surface position (see Fig. 2), where a less organised copper film structure is observed. In contrast to the first case, the cross-section in Fig. 2 shows recrystallised domains that are only partially constrained by the localised contamination layers. These larger Cu domains might result from either non-uniform incorporation of contaminants during deposition or from its disruption upon post-deposition recrystallisation.

The chemical composition of such layered samples, *i.e.*, the alternation of large recrystallised Cu domains and narrow transition layers within the same copper deposit, derived from LIMS measurements is presented in Fig. 3. Both panels (a) and (b) display the recorded Cu signal together with the major elements of the Imep additive (C, N, O, and S). Their abrupt intensity changes are in good agreement with the observations of narrow transition layers in the FIB measurements (Fig. 1 and 2). Whereas in panel (a) of Fig. 3 a sharp increase of the major elements for all transition layers is observed, matching the uniform and stable Cu deposition process similar to situation in Fig. 1, in panel (b) of Fig. 3 only few transitions are detected, analogous to the second situation shown in Fig. 2. The chemical analysis shows massive incorporation of contaminants inside these transition layers of more than 35 000 ppm. However, inside well recrystallised copper domains only trace amounts of impurities at the level of about 150 ppm are detected. Additionally, as observed in Fig. 3b, there are occasions where a relatively large amount of impurities are randomly distributed between well-localised contaminated transition layers (see blue shaded areas). These impurities, amounting to ~1000 ppm, originate from localised transition layers that might be displaced by post-deposition recrystallisation across the initial

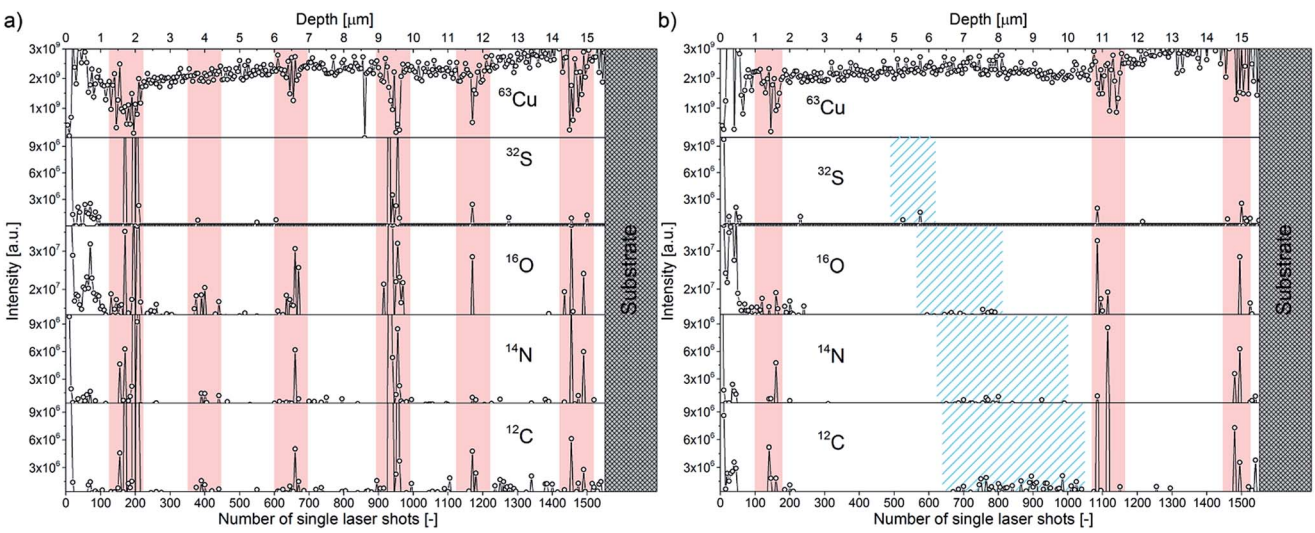

Fig. 3 Mass spectrometric analysis by LIMS. The chemical analysis of additive-assisted electrodeposited Cu films at high depth resolution on two different sample locations is shown. Panel (a): all expected transition layers, highlighted by pink bars, were recorded by the LIMS measurements (situation analogue to sample locations as illustrated in Fig. 1). Panel (b): only three of six transitions are visible (situation analogue to sample locations as illustrated in Fig. 2).

transition layers (yellow dotted line in Fig. 2). Hence, the detection of contamination fluctuations in the lower micrometre range within a solid material is not restricted anymore to visual microscopic techniques but can be directly measured and quantified over a large vertical distance by the presented mass spectrometric technique.

For the first time, using the LIMS depth profiling technique, it is possible to identify and to quantify chemical inhomogeneities at the grain size level and at their boundaries, the narrow transition layers, over a large vertical range. This remarkable capability is attributed to the high vertical resolution (in the nm range) and the high detection sensitivity of the presented LIMS instrument, which enables measurements with a low ablation rate that causes minimal erosion damage and avoids vertical mixing over large sample depths. The gathered chemical data together with the results from FIB micrographs allow new and detailed insights of the elemental composition of the sample material. The presented studies underline the suitability of Imep-based chemistry for Damascene applications in the semiconductor industry. The LIMS measurement demonstrated the low embedment of the additives inside recrystallised Cu domains, while the location of additives is mostly restricted to the narrow transition layers between the Cu domains. By optimising the growth of the recrystallised Cu domains, the total inclusion of additives in a device can be minimised. This high depth resolution chemical analysis is crucial to support the further improvement of the bottom-up fill process used in the semiconductor industry and hence, for the increased performance of nowadays microchip devices.

The presented instrument with its capabilities is equally suited for many other fields of research, where instrument characteristics such as detection sensitivity and quantitative depth profiling with high spatial resolution are required. This includes *e.g.* the analysis of vertical profiles of solar cells,[12] investigations of space weathered samples,[28] and the monitoring of phase transitions in fossilized sample materials,[29] among many others.

Acknowledgements

This work is supported by the Swiss National Science Foundation.

Notes and references

1 P. C. Andricacos, C. Uzoh, J. O. Dukovic, J. Horkans and H. Deligianni, *IBM J. Res. Dev.*, 1998, **42**, 567.
2 T. P. Moffat, D. Wheeler, M. D. Edelstein and D. Josell, *IBM J. Res. Dev.*, 2005, **49**, 19.
3 R. Akolkar, C.-C. Cheng, R. Chebiam, A. Fajardo and V. Dubin, *ECS Trans.*, 2007, **2**, 13.
4 K. Schuegraf, M. C. Abraham, A. Brand, M. Naik and R. Thakur, *J. Electron Devices Soc.*, 2013, **1**, 66.
5 J. P. Gambino, S. A. Adderly and J. U. Knickerbocker, *Microelectron. Eng.*, 2015, **135**, 73.
6 R. Akolkar and U. Landau, *J. Electrochem. Soc.*, 2004, **151**, C702.
7 J. D. Reid and J. Zhou, *ECS Trans.*, 2007, **2**, 77.
8 J. S. Becker, *Inorganic Mass Spectrometry – Principles and Applications*, John Wiley & Sons Ltd., England, 2007.
9 J. Pantoja-Enríquez, E. Gómez-Barojas, R. Silva-González and U. Pal, *Sol. Energy Mater. Sol. Cells*, 2007, **91**, 1392.
10 M. Duta, S. Mihaiu, C. Munteanu, M. Anastasescu, P. Osiceanu, A. Marin, S. Preda, M. Nicolescu, M. Modreanu, M. Zaharescu and M. Gartner, *Appl. Surf. Sci.*, 2015, **344**, 196.
11 N. T. M. Hai, D. Lechner, F. Stricker, J. Furrer and P. Broekmann, *ChemElectroChem*, 2015, **2**, 664.
12 J. Pisonero, N. Bordel, C. Gonzalez de Vega, B. Fernández, R. Pereiro and A. Sanz-Medel, *Anal. Bioanal. Chem.*, 2015, **405**, 5655.
13 A. Gutiérrez-González, C. González-Gago, J. Pisonero, N. Tibbetts, A. Menéndez, M. Vélez and N. Bordel, *J. Anal. At. Spectrom.*, 2015, **30**, 191.
14 S. J. M. van Malderen, J. T. van Elteren and F. Vanhaecke, *Anal. Chem.*, 2015, **87**, 6125.
15 V. Grimaudo, P. Moreno-García, A. Riedo, M. B. Neuland, M. Tulej, P. Broekmann and P. Wurz, *Anal. Chem.*, 2015, **87**, 2037.
16 M. Tulej, A. Riedo, M. B. Neuland, S. Meyer, P. Wurz, N. Thomas, V. Grimaudo, P. Moreno-García, P. Broekmann, A. Neubeck and M. Ivarsson, *Geostand. Geoanal. Res.*, 2014, **38**, 441.
17 M. B. Neuland, S. Meyer, A. Riedo, M. Tuej, P. Wurz and K. Mezger, *Planet. Space Sci.*, 2014, **101**, 196.
18 A. Riedo, S. Meyer, B. Heredia, M. Neuland, A. Bieler, M. Tulej, I. Leya, M. Iakovleva, K. Mezger and P. Wurz, *Planet. Space Sci.*, 2013, **87**, 1.
19 A. Riedo, M. Neuland, S. Meyer, M. Tulej and P. Wurz, *J. Anal. At. Spectrom.*, 2013, **28**, 1256.
20 A. Riedo, A. Bieler, M. Neuland, M. Tulej and P. Wurz, *J. Mass Spectrom.*, 2013, **48**, 1.
21 A. Bieler, K. Altwegg, L. Hofer, A. Jäckel, A. Riedo, T. Sémon and P. Wurz, *J. Mass Spectrom.*, 2011, **46**, 1143.
22 U. Rohner, J. Whitby and P. Wurz, *Meas. Sci. Technol.*, 2003, **14**, 2159.
23 B. Zhang, M. He, W. Hang and B. Huang, *Anal. Chem.*, 2013, **85**, 4507.
24 N. T. M. Hai, J. Odermatt, V. Grimaudo, K. W. Krämer, A. Fluegel, M. Arnold, D. Mayer and P. Broekmann, *J. Phys. Chem. C*, 2012, **116**, 6913.
25 N. T. M. Hai, K. W. Krämer, A. Fluegel, M. Arnold, D. Mayer and P. Broekmann, *Electrochim. Acta*, 2012, **83**, 367.
26 K. Krischer, N. Mazouz and P. Grauel, *Angew. Chem., Int. Ed.*, 2001, **40**, 850.
27 P. Strasser, M. Eiswirth and M. T. M. Koper, *J. Electroanal. Chem.*, 1999, **478**, 50.
28 T. Noguchi, T. Nakamura, M. Kimura, M. E. Zolensky, M. Tanaka, T. Hashimoto, M. Konno, A. Nakato, T. Ogami, A. Fujimura, M. Abe, T. Yada, T. Mukai, M. Ueno, T. Okada, K. Shirai, Y. Ishibashi and R. Okazaki, *Science*, 2011, **333**, 1121.
29 M. Tulej, A. Neubeck, M. Ivarsson, A. Riedo, M. B. Neuland, S. Meyer and P. Wurz, *Astrobiology*, 2015, **15**, 669.

